DOI: 10.55522/jmpas.V11I5.3957 ISSN NO. 2320–7418

International peer reviewed open access journal

Journal of Medical Pharmaceutical and Allied Sciences

Journal homepage: www.jmpas.com CODEN: JMPACO

Research article

In silico screening and identification of leads against multi-targets of type II diabetes in *Plectranthus vettiveroides*

Remya RP, Sreekumar S*, Biju CK

Biotechnology and Bioinformatics Division, Saraswathy Thangavelu Extension Centre, KSCSTE-Jawaharlal Nehru Tropical Botanic Garden and Research Institute, A Research Centre of University of Kerala, Puthenthope, Thiruvananthapuram, India.

ABSTRACT

Generally, phytochemicals have activity on multi-targets and such molecules have been used as effective drugs against the diseases caused by multi-factorial causation like diabetes mellitus (DM). *Plectranthus vettiveroides* (Jacob) N.P. Singh & B.D. Sharma has been used as a polychrest against various diseases including type II diabetes in tradition system of medicine. The present investigation aimed to validate anti-diabetic property of the root derived essential oil of *P. vettiveroides* and identification of leads with activity on six targets of DM through *in silico* method. A total of 78 phytochemicals determined through Gas chromatography –mass spectrometry (GC-MS) analysis of the essential oil were docked with each of the six selected targets namely 11β-hydroxysteroid dehydrogenase type 1, dipeptidyl peptidase IV, protein-tyrosine phosphatase 1B, human pancreatic alpha-amylase, human lysosomal acid-alpha-glucosidase, and phosphorylated insulin receptor tyrosine kinase. The structures of the phytochemicals were retrieved from PubChem and the targets were retrieved from Protein Data Bank (PDB). Docking was carried out in AutoDockVina and the molecules with free energy of binding ≤-6 kcal/mol were considered as hit molecule. Out of 78 phytochemicals screened, 39 have activity on all the tested targets. Based on the docking interaction, drug-likeness and absorption, distribution, metabolism, excretion and toxicity (ADMET) property the best lead molecule against each target were determined. The overall results revealed that basically majority of the hits are terpinoides and not induced any toxicity. Therefore, the oil as such can be recommended as medicament against DM, since the individual, synergistic and cumulative effect of phytochemicals may concomitantly inhibit multi-targets of DM and act as an effective drug.

Keywords: *Plectranthus vettiveroides*, Anti-diabetes, Diabetes mellitus, Phytochemicals, Molecular docking.

Received - 02-07-2022, Accepted- 12-09-2022

Correspondence: Sreekumar S ✉ drsreekumar@rediffmail.com, **Orcid Id**: 0000-0002-9488-0277

Biotechnology and Bioinformatics Division, Saraswathy Thangavelu Extension Centre, KSCSTE-Jawaharlal Nehru Tropical Botanic Garden and Research Institute, Puthenthope, Thiruvananthapuram, India.

INTRODUCTION

Diabetes Mellitus (DM) is a combination of heterogeneous disorders characterized by elevated glucose levels in the blood resulting from a defect in insulin secretion, insulin action, or both [1-3]. According to the International Diabetes Federation (2021) globally 537 million people with age group 20-79 years are living with diabetes, i.e., 1 in 10 and it is predicted to rise to 643 million by 2030, and 783 million by 2045. It is responsible for 6.7 million deaths in 2021, i.e., 1 every 5 seconds. In India, 74.2 million people of the age group 20-79 years have diabetes. India accounts for 1 in 7 of all adults living with diabetes in the world [4]. DM are two types, insulin-dependent or type 1 and insulin non-dependent or type II [5]. Type 1 DM is recognized as juvenile diabetes, which is an autoimmune disorder characterised by the loss of insulin-producing pancreatic β-cells that leads to hyperglycemia [6]. Exogenous insulin therapy is essential to prevent fatal complications of type 1 DM [7]. Type II DM accounts for more than 95% of all cases of diabetes and it is strongly associated with lifestyle factors and genetics [8,9]. Its underlying defects can vary from predominant insulin resistance with relative insulin deficiency to a predominant insulin secretary defect with insulin resistance [10]. Type II DM can be managed by using drugs and lifestyle modifications. Several classes of oral anti-hyperglycemic agents have been used in pharmacotherapy [11]. The side effects associated with the prolonged use of the available DM drugs necessitated a quest for safe and effective drugs, especially those of plant origin [12], which are synthesized within the living system by repeated testing and modification as part of the long-term evolutionary process [13]. In traditional systems of medicine, many plant species have been used as anti-diabetic agents [14].

Plectranthus vettiveroides (Jacob) N.P. Singh & B.D. Sharma, belonging to the family Lamiaceae, has been used as a

polychrest in Indian traditional treatment system against several ailments, including diabetes [15]. It is an herbaceous, endemic to south Indian, root-derived essential oil yielding plant. It has deep straw-coloured hair like aromatic fibrous roots, which has been used individually or as an ingredient of over 75 herbal preparations marketed by leading herbal drug manufactures [16]. The plant has been extinct in the wild and its cultivation is currently limited in Kollidam in Cuddallore district, Tamil Nadu, by a few farmers who want to fulfill their traditional customs and beliefs [17]. The plant needs moist sandy soil, open sunlight and specific agro-climatic conditions and, therefore, its extended cultivation is limited. In this backdrop, due to the scarcity of genuine raw material, the drug manufacturers are using adulterants/substitutes that might adversely affect the quality of the drug [18]. To address this problem, identification of individual chemical constituents of the essential oil and its therapeutic activities attain prime importance. Moreover, many authors have demonstrated the multi-target activity of plant-derived compounds [19,20]. It is well acknowledged that diseases caused by multi-factorial causation like diabetes phyto molecules are the best remedy, since many phytochemicals have concomitant activity on multi-targets of pathogenicity and effectively control/prevent the disease. Hence, the present investigation aimed to find out the individual chemical constituents of the *P. vettiveroides* root derived essential oil, evaluate anti-diabetes activity of each phytochemical and find out lead molecules with inhibitory activity on multi-targets of type II diabetes through *in silico* method.

MATERIALS AND METHODS

Phytochemical Screening

Extraction of Essential Oil and GC-MS Analysis

The fresh roots from 70-80 day old plants cultivated following the standardised agrotechnology package of practice at Saraswathy Thangavelu Extension Centre of Jawaharlal Nehru Tropical Botanic Garden and Research Institute, Puthenthope, Thiruvananthapuram, located near the coastal area of the Arabian Sea, where the sandy soil and agroclimatic condition almost similar to its native habitat were used for oil extraction [17]. The roots harvested from the foregoing plants were thoroughly washed with tap water to remove all soil particles and other impurities. They were kept on blotting paper for removing the water drops from the surface of the roots and 50 g fresh roots was hydro distilled in 500 ml distilled water for 6.00 h using Clevenger apparatus. The distillate was extracted with diethyl ether, dried over anhydrous sodium sulphate, determined total yield and stored at 4 ^{0}C.

The GC-MS analysis of the essential oil was carried out on Agilent 5975 Inert XL MSD coupled with 7890 A gas chromatograph (Agilent, Waldbronn, Germany) using a split-splitless injector. The injector temperature was adjusted to 250°C. The splitless time was 1 min, while the split ratio was 50:1. Helium was used as a carrier gas at velocity 1.0 ml min^{-1}. The ion source, quadrupole and transfer line temperatures were maintained at 230°C, 150°C and 250°C, respectively. Chemstation (Agilent) was used to acquire the chromatographic data and mass spectrum library NIST 2005 (Gatesburg, USA) to identify the compound. The 30 m × 0.25 mm × 0.25 µm capillary column Db- 5MS was used. The oven temperature program was as follows: initially 40 °C held for 5 min, then ramped 7°C min-^{1} to 280°C, held for 10 min. The molecular weight and structure of the test materials were ascertained by interpreting the mass spectrum of GC-MS using the National Institute Standard and Technology (NIST) database [21]. The mass spectrum of the unknown component was compared with the spectrum of the known components stored in the NIST library and determined the molecular weight and structure of the components of the test materials [22].

In Silico Screening

Type II DM is caused by multi-factorial causation and therefore, six potential targets which have pivotal roles in the disease cycle have been selected as the targets.

Preparation of Targets

The crystal structures of the six target proteins namely11β-hydroxysteroid dehydrogenase type 1 (11β-HSD1, PDB ID: 1XU7), Dipeptidyl peptidase IV (DPP IV, PDB ID: 1PFQ) Protein-tyrosine phosphatase 1B (PTP1B, PDB ID : 2QBQ), Human pancreatic alpha-amylase (PDB ID: 2QV4), Human lysosomal acid-alpha-glucosidase (PDB ID: 5NN8), and Phosphorylated insulin receptor tyrosine kinase (PDB ID:1IR3) were retrieved from Protein Data Bank. Prior to docking, from each target all water molecules were removed, added polar hydrogen atoms and gasteiger charges, and converted to pdbqt file format using AutoDock. The structural details of target proteins were analyzed using VADAR (Volume, Area, Dihedral Angle Reporter) web server following the method of Willard et al., (2003) and active sites were determined using Swiss Protein Viewer, SPDBV [23,24].

Selection and Preparation of Ligands

A total of 78 phytochemicals from root derived essential oil of *P. vetteveroides* were selected as ligands. Canonical SMILES notations of these phytochemicals were procured from Pubchem (pubchem.ncbi.nlm.nih.gov/) and converted to the PDB format using the tool CORINA [25,26].

Molecular Docking

It was performed using the tool AutoDock Vina following the standard method [27]. The ligands were docked individually to each receptor with grid coordinates (grid center) and grid boxes of convenient sizes were assigned to each receptor. Docking input files were created using Auto Dock. The ligand was in a flexible condition when interacting with macro-molecules under rigid conditions. The

configuration file was prepared by opening notepad to run Auto Dock Vina and prepared grid box having the different X, Y and Z coordinates values for each receptor molecule where the ligand molecule is to be docked. Ligand-binding affinities were predicted as negative Gibbs free energy (ΔG) scores (kcal/mol), which were calculated on the basis of the Auto Dock Vina scoring function. The docked complex forming hydrogen bonds and other parameters like inter-molecular energy (kcal/mol) and inhibition constant (μM) were analyzed by Auto dock tool. Ten best poses were generated for each ligand and scored using Auto dock Vina scoring functions. Based on the least binding energy level ligands were ranked. Post-docking analyses were visualized using PyMOL and Discovery Studio Biovia 2017.

Post Docking Analysis

The top ranked five hit molecules obtained against the selected target proteins were further analysed for the absorption, distribution, metabolism, elimination and toxicity (ADMET) using pkCSM server. The drug-likeness properties were predicted using the online tool Mol Soft by uploading the structures of the selected phytochemicals in SMILES format [28].

RESULTS AND DISCUSSION

Phytochemical Screening

The essential oil of *P. vettiveroides* obtained by hydro-distillation of fresh roots had a bright orange red colour, highly viscous with a pleasant odour and total yield from the fresh root was 0.4% w/w. The GC-MS analysis is the standard method that has been increasingly applied for the analysis of medicinal plants for non-polar components such as volatile oil, fatty acids and alkaloid [29]. The GC-MS chromatogram of the root-derived essential oil (Figure 1) indicated that the essential oil is a combination of monocyclic and bicyclic sesqui-terpenoids, polycyclic hydrocarbons and fatty acids esters. A total of 78 compounds were identified comparing the data available in the NIST library. It constitutes 83.29% w/w of the total oil, while 16.71% w/w of the oil constituents remains as unidentified. Among the identified 78 phytochemicals, the most abundant compounds were myrtenyl acetate (16.82% w/w) and farnesyl acetate (15.91% w/w). These two compounds represented 32.73% w/w of the total oil. The other major compounds in the order of merit was (3S,4R,5R,6R)-4,5-bis(hydroxymethyl)-3,6-dimethylcyclohexene (4.32% w/w), 4,4-dimethyl-3-(3-methylbut-enylidene)-2-methylenebicyclo[4.1.0]heptane(4.08% w/w), 4,6,6-trimethyl-2-(3-methylbuta-1,3-dienyl) oxatricyclo [5.1.0.0(2,4)]octane (3.90% w/w), valancene (2.80% w/w), and calarene (2.41% w/w). All the remaining compounds contribute only less than 2% w/w. The GC-MS chromatogram of the root-derived essential oil is depicted in Figure 1 and the list of identified phytochemical components were listed in Table 1.

Figure 1: The GC-MS chromatogram of the root derived essential oil of *P. vettiveroides*

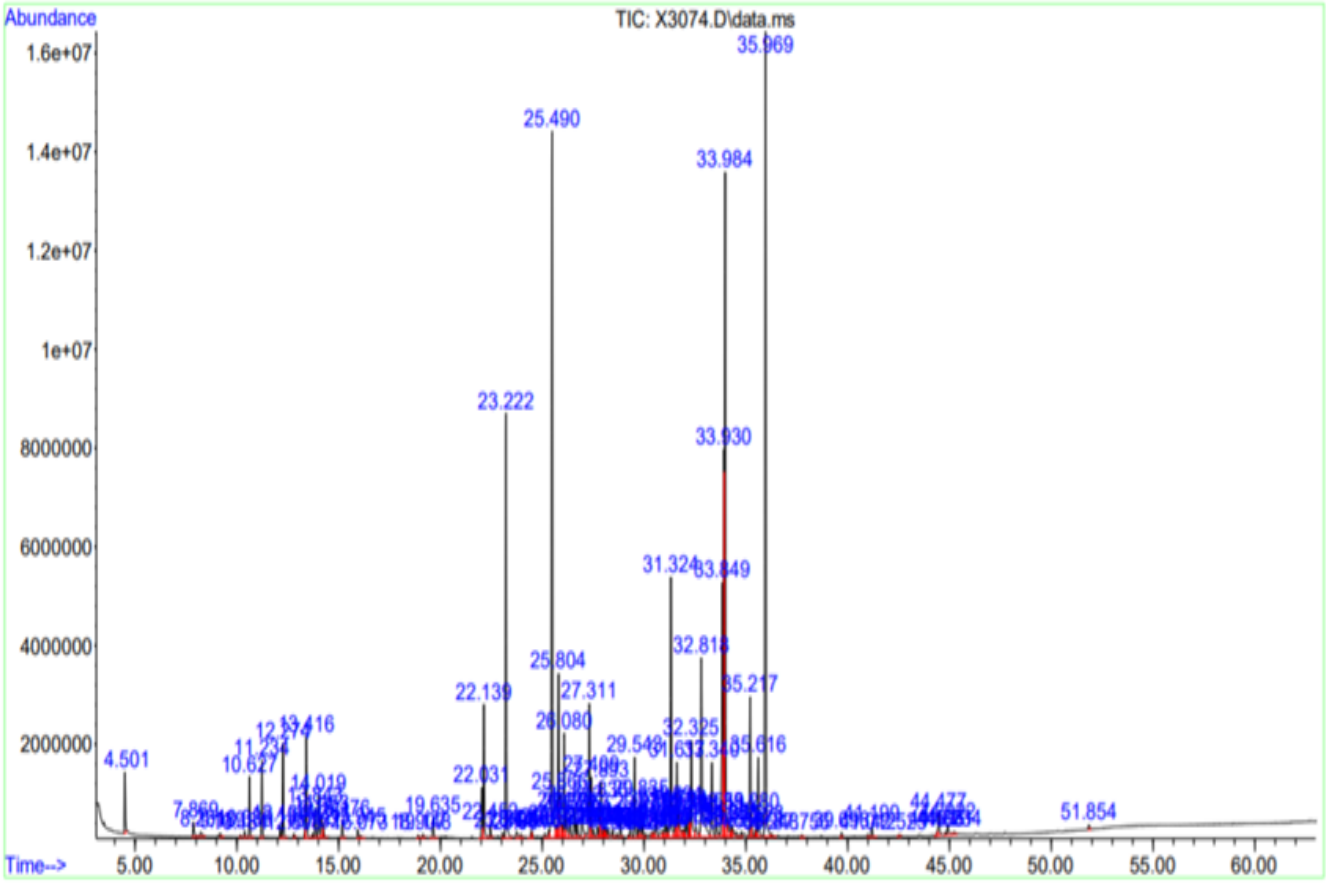

Table 1: The list of phytochemicals identified from root-derived essential oil of *P. vettiveroides* and the docking score of each compound against the selected targets such as11β-hydroxysteroid dehydrogenase type 1 (11β-HSD1, PDB ID: 1XU7), Dipeptidyl peptidase IV (DPP IV, PDB ID: 1PFQ) Protein-tyrosine phosphatase 1B (PTP1B, PDB ID : 2QBQ), Human pancreatic alpha-amylase (PDB ID: 2QV4), Human lysosomal acid-alpha-glucosidase (PDB ID: 5NN8), and Phosphorylated insulin receptor tyrosine kinase (PDB ID:1IR3)

Phytochemicals determined through GC-MS			Target PDB ID and binding energy (kcal/mol)					
Phytochemicals	**RT**	**% of total (w/w)**	**1 X U 7**	**1 P F Q**	**2 Q B Q**	**2 Q V 4**	**5 N N 8**	**1 I R 3**
α-thujene ($C_{10}H_{16}$)	10.39	0.09	-5	-5.4	-5.8	-5.6	-6.1	-5
α-Pinene ($C_{10}H_{16}$)	10.63	0.79	-5.1	-5.2	-6.3	-5.1	-5.8	-4.7
Camphene ($C_{10}H_{16}$)	11.23	0.99	-5	-5.5	-5.9	-5	-5.6	-4.7
β-Phellandrene ($C_{10}H_{16}$)	12.13	0.17	-5.1	-5.8	-6	-5.5	-6.2	-5.2
β-Pinene ($C_{10}H_{16}$)	12.27	1.27	-5	-5.3	-6.1	-5.1	-5.9	-4.9
α-Phellandrene ($C_{10}H_{16}$)	13.35	0.09	-4.9	-5.5	-5.7	-5.4	-5.6	-4.6
3-Carene ($C_{10}H_{16}$)	13.42	1.45	-5.3	-5.8	-6	-5.4	-6.4	-5.6
3-Methylene-1,5,5-trimethylcyclohexene ($C_{10}H_{16}$)	13.73	0.06	-5.3	-5.5	-5.7	-5.3	-6.3	-5
P-Cymene ($C_{10}H_{16}$)	13.84	0.43	-5.4	-6.1	-6	-5.5	-6	-5
O-Cymene ($C_{10}H_{16}$)	14.02	0.67	-5.1	-5.8	-5.9	-5.5	-6.3	-5.2
Limonene ($C_{10}H_{16}$)	14.16	0.39	-5.4	-5.7	-6	-5.3	-6.2	-5.2
Eucalyptol ($C_{10}H_{18}O$)	14.25	0.21	-4.9	-5.1	-6.2	-5.3	-5.9	-4.9
γ-terpinene ($C_{10}H_{16}$)	15.18	0.29	-5.4	-6.3	-6.1	-5.4	-6.1	-5.3
Terpinolene ($C_{10}H_{16}$)	15.95	0.21	-5.3	-6	-6.3	-5.5	-6.3	-5.2
Borneol ($C_{10}H_{18}O$)	18.91	0.05	-5.6	-5	-6	-5.1	-5.8	-4.6
(-)-4-Terpineol ($C_{10}H_{18}O$)	19.15	0.07	-5.9	-6.1	-6.3	-5.3	-6.2	5.1
Myrtenol ($C_{12}H_{18}O_2$)	19.64	1.14	-5.5	-5.7	-6.5	-5.5	-6	-4.9
Bornyl acetate ($C_{12}H_{18}O_2$)	22.14	1.84	-5.5	-5.5	-7	-6.1	-6.8	-5.2
(-)-trans-Pinocarvyl acetate ($C_{12}H_{18}O_2$)	22.45	0.19	-5.5	-6	-7.5	-6.2	-7.2	-6
Myrtenylacetate ($C_{12}H_{18}O_2$)	25.49	16.82	-5.9	-6.4	-7.5	-5.9	-6.8	-5.4
Perillyl acetate ($C_{12}H_{18}O_2$)	23.75	0.18	**-6.2**	**-6.5**	**-7.4**	**-6.3**	**-6.5**	**-6**
α-Longipinene ($C_{15}H_{24}$)	23.96	0.11	**-6.9**	**-6.3**	**-8.5**	**-6.8**	**-7.5**	**-6.2**
Ylangene ($C_{15}H_{24}$)	24.46	0.09	**-6.5**	**-6.6**	**-8**	**-6.9**	**-7**	**-6.4**
Naphthalene, 1,2,3,5,8,8a-hexahydro ($C_{10}H_{14}$)	24.51	0.08	-5.3	-5.9	-6.2	-5.7	-6.6	-5.3
Cuminyl acetate ($C_{12}H_{16}O_2$)	25.14	0.12	**-6**	**-6.9**	**-7.4**	**-6.4**	**-7.1**	**-6.2**
Benzenebutanal, γ,4-dimethyl ($C_{12}H_{16}O$)	25.33	0.16	-5.7	-6.1	-6.7	-5.6	-5.7	-5.5
Caryophyllene ($C_{15}H_{24}$)	25.7	0.20	-6.7	-6.2	-6.5	-7.4	-6.8	-5.8
Calarene ($C_{15}H_{24}$)	25.84	2.41	-6.7	-6.2	-5.7	-6.7	-7.2	-5.7
Valencene ($C_{15}H_{24}$)	25.87	2.80	-6.3	-6.2	-7.5	-6.7	-6.5	-5.8
Isolongifolene, 9,10-dehydro ($C_{15}H_{22}$)	26.08	1.43	**-6.7**	**-6.5**	**-6.8**	**-6.8**	**-7.4**	**-6.2**
alpha-Himachalene ($C_{15}H_{24}$)	26.18	0.58	**-6.9**	**-6.9**	**-7.4**	**-7**	**-8.6**	**-6.2**
α-Caryophyllene ($C_{15}H_{24}$)	26.37	0.42	-6.8	-6.4	-6.8	-7.2	-6.5	-5.9
(+)-3-Carene, 10-(acetylmethyl) ($C_{13}H_{20}O$)	26.59	0.59	**-6.1**	**-6.1**	**-7.6**	**-6.6**	**-7**	**-6.1**
Longifolene-(V4) ($C_{15}H_{24}$)	26.72	0.27	-6.3	-6.7	-5.8	-6.7	-7.2	-5.1
Isocaryophillene ($C_{15}H_{24}$)	26.95	0.60	-6.7	-6.2	-6.3	-7.4	-7.1	-5.9
beta-Himachalene ($C_{15}H_{24}$)	27.41	0.17	-7	-6.6	-6	-7.2	-7.7	-5.7
2H-1-Benzopyran, 3,5,6,8a-tetrahydro-2,5,5,8a-tetramethyl-, trans ($C_{13}H_{20}O$)	27.72	0.20	-5.9	-6.1	-7.2	-6.1	-7.2	-5.8
Naphthalene, 1,2,3,4-tetrahydro-1,6-dimethyl-4-(1-methylethyl)-, (1S-cis) ($C_{15}H_{22}$)	27.84	0.47	**-6.8**	**-7.3**	**-6.5**	**-6.8**	**-8**	**-6.6**

Delta-Amorphene ($C_{15}H_{24}$)	27.89	0.82	**-6.5**	**-7.3**	**-6.6**	**-7.1**	**-7.4**	**-6.2**
2-(4a,8-Dimethyl-2,3,4,4a,5,6-hexahydro-naphthalen-2-yl)-prop-2-en-1-ol ($C_{15}H_{22}O$)	28.01	0.10	**-7.2**	**-7.1**	**-7.2**	**-7.3**	**-8**	**-6.2**
Cycloisolongifolene, 9,10-dehydro- ($C_{15}H_{22}$)	28.06	0.47	**-6.6**	**-6.4**	**-6.3**	**-6.9**	**-7**	**-6.2**
α-Calacorene ($C_{15}H_{20}$)	28.13	0.28	**-6.8**	**-7**	**-7.4**	**-7.4**	**-7.4**	**-6.4**
Eudesm-7(11)-en-4-ol ($C_{15}H_{26}O$)	28.26	0.23	**-6.9**	**-6.8**	**-7.3**	**-6.9**	**-7.6**	**-6.5**
(-)-Spathulenol ($C_{15}H_{24}O$)	28.84	0.23	-6.9	-6.6	-5.8	-7.1	-6.8	-6
Caryophyllene oxide ($C_{15}H_{24}O$)	29.25	0.05	**-6.8**	**-6.7**	**-6**	**-7.3**	**-6.6**	**-6.2**
(-)-Globulol ($C_{15}H_{26}O$)	29.34	0.22	-6.7	-6.4	-5.9	-7.1	-6.8	-6.2
Icosapent methyl ($C_{21}H_{32}O_2$)	29.54	1.18	-6.1	-6.6	-6.5	-6.2	-6.2	-5.3
8-Isopropenyl-1,3,3,7-tetramethyl-bicyclo [5.1.0] oct-5-en-2-one ($C_{15}H_{22}O$)	29.72	0.21	-6.5	-6.3	-5.5	-6.7	-6.6	-5.7
1-(2,4-Dimethylphenyl)-3-(tetrahydrofuryl-2) propane ($C_{15}H_{22}O$)	29.84	0.56	-6.3	-6.6	-7.7	-6.6	-6.8	-5.6
Bicyclo[4.4.0]dec-5-ene, 1,5-dimethyl-3-hydroxy-8-(1-methylene-2-hydroxyethyl-1) ($C_{15}H_{24}O2$)	29.94	0.35	**-7.4**	**-7.2**	**-7.4**	**-7.3**	**-8**	**-6.6**
5β,7βH,10α-Eudesm-11-en-1α-ol ($C_{15}H_{26}O$)	30.05	0.07	**-6.9**	**-6.5**	**-7.2**	**-6.6**	**-6.3**	**-6.3**
Cubenol ($C_{15}H_{26}O$)	30.37	0.54	-6.7	-7	-5.4	-7	-7.2	-6.2
4-(1-Adamantanecarboxamido)-2-ethyl-6-methyl-3-pyridyl 1-adamantanecarboxylate ($C_{30}H_{40}N_2O_3$)	30.48	0.41	**-9.8**	**-8.3**	**-7.3**	**-8.7**	**-8.1**	**-8.1**
(3S,4R,5R,6R)-4,5-Bis(hydroxymethyl)-3,6-dimethylcyclohexene ($C_{10}H_{18}O_2$)	30.61	4.32	-5.2	-5.1	-6.6	-5.5	-6	-5.1
α-Bisabolol ($C_{15}H_{26}O$)	30.83	1.33	**-6.7**	**-6.9**	**-8**	**-6.4**	**-6.8**	**-6.2**
Alpha cadinol ($C_{15}H_{26}O$)	30.95	1.30	**-6.9**	**-6.6**	**-6**	**-7**	**-7.5**	**-6**
6-(1-Hydroxymethylvinyl)-4,8a-dimethyl-3,5,6,7,8,8a-hexahydro-1H-naphthalen-2-one ($C_{15}H_{22}O2$)	31.71	0.65	**-7.3**	**-6.8**	**-6**	**-7.2**	**-8.1**	**-6.7**
4,4-Dimethyl-3-(3-methylbut-3-enylidene)-2-methylenebicyclo [4.1.0] heptane ($C_{15}H_{22}$)	31.91	4.08	**-6.3**	**-6.5**	**-6.4**	**-7.1**	**-7.1**	**-6**
γ-Gurjunenepoxide-(2) ($C_{15}H_{24}O$)	32.21	0.23	**-6.7**	**-7.2**	**-6.8**	**-7.3**	**-6.9**	**-6.9**
Acetic acid, 3-hydroxy-6-isopropenyl-4,8a-dimethyl-1,2,3,5,6,7,8,8a-octahydronaphthalen-2-ylester ($C_{17}H_{26}O_3$)	32.25	0.32	-7.1	-6.7	-5.8	-7.4	-6.9	-6.1
5(1H)-Azulenone, 2,4,6,7,8,8a-hexahydro-3,8-dimethyl-4-(1-methylethylidene)-, (8S-cis) ($C_{15}H_{22}O$)	32.33	1.72	**-6.5**	**-6.4**	**-6.5**	**-6.8**	**-6.3**	**-6.1**
Longipinocarvone ($C_{15}H_{22}O$)	32.56	0.32	**-7.1**	**-6.5**	**-6.6**	**-7.1**	**-7.7**	**-6.4**
Aromadendrene, dehydro ($C_{15}H_{22}$)	33.34	1.59	**-7.3**	**-6.8**	**-6.9**	**-6.9**	**-7.4**	**-6.7**
4,6,6-Trimethyl-2-(3-methylbuta-1,3-dienyl)-3-oxatricyclo [5.1.0.0(2,4)] octane ($C_{15}H_{22}O$)	33.85	3.90	**-7**	**-6.7**	**-6.7**	**-6.5**	**-7.4**	**-5.8**
Farnesyl acetate($C_{17}H_{28}O_2$)	33.93	15.91	-5.8	-6.4	-7.4	-6.2	-6.3	-5.8
6-(1,3-Dimethyl-buta-1,3-dienyl)-1,5,5-trimethyl-7-oxa-bicyclo [4.1.0] hept-2-ene ($C_{15}H_{22}O$)	34.34	0.20	-6	-5.7	-5.6	-6.5	-6.3	-5.5

Acetate, [6-(acetyloxy)-5,5,8a-trimethyl-2-methyleneperhydro-1-naphthalenyl] methyl ester ($C_{19}H_{30}O_4$)	35.28	0.34	**-7.4**	**-7.4**	**-6.1**	**-7.5**	**-7.5**	**-7**
Bicylo[4.1.0]heptane, 7-bicyclo[4.1.0]hept-7-ylidene ($C_{14}H_{20}$)	35.52	0.15	**-6.4**	**-6.4**	**-8.6**	**-6.4**	**-6.2**	**-6.3**
Methyl hinokiate ($C_{16}H_{24}O_2$)	35.62	1.22	**-7**	**-6.9**	**-6.4**	**-7.2**	**-7.2**	**-6**
1,1,4a-Trimethyl-5,6-dimethylenedecahydronaphthalene ($C_{15}H_{24}$)	36.25	0.10	**-6.7**	**-6.4**	**-6.6**	**-7.5**	**-7.9**	**-6.3**
cis-Nuciferol ($C_{15}H_{22}O$)	37.76	0.05	-5.8	-6.7	-7.8	-6.3	-6.7	-6.4
Dehydroabietan ($C_{20}H_{30}$)	39.7	0.07	**-8.3**	**-8.4**	**-8.2**	**-9.1**	**-8.8**	**-7.5**
1,4-Methanoazulene-9-methanol, decahydro-4,8,8-trimethyl-, [1S-(1α,3aβ,4α,8aβ,9R*)] ($C_{15}H_{26}O$)	41.01	0.06	-6.6	-6.1	-6.3	-6.5	-6.5	-5.9
Sclareol ($C_{20}H_{36}O_2$)	41.2	0.18	-7.3	-7.3	-5.6	-7.5	-7.5	-6.2
Trans-totarol ($C_{20}H_{30}O$)	44.48	0.42	-8.2	-7.7	-5.6	-8	-9.2	-6.9
Larixol ($C_{20}H_{34}O_2$)	44.8	0.05	**-7.2**	**-7.3**	**-6.2**	**-7.5**	**-7.3**	**-6.5**
Dronabinol	44.92	0.26	**-8.2**	**-7.7**	**-8.5**	**-8.5**	**-7.9**	**-7.4**
Squalene ($C_{30}H_5O$)	51.85	0.08	**-7**	**-7.3**	**-7.2**	**-6.9**	**-7.2**	**-4.8**

In *P. vettiveroides* a total of 38 phytochemicals were reported by Saraswathy et al. [30] and 62 by Sailaja et al. [31]. While in the present study 78 phytochemicals were identified. Significant differences in percentage occurrence of individual components were noted when compared the present and earlier reports. Five compounds namely myrtenyl acetate, α-bisabolol, myrtenol, (-)-globulol and caryophyllene oxide reported earlier was also found in the present investigation but its percentage occurrence differed significantly [30,31]. Twenty compounds were common when compared the present result with the report of Sailaja et al. [31].

Based on the percentage occurrence the major compounds which were present more than 2% w/w in the present study in the order of merit was myrtenyl acetate (16.82% w/w), farnesyl acetate (15.91% w/w), (3S,4R,5R,6R)-4,5-bis (hydroxymethyl)-3,6-dimethylcyclohexene (4.32% w/w), 4,4-dimethyl-3-(3-methylbut-3-enylidene) -2-methylenebicyclo[4.1.0] heptane (4.08% w/w), 4,6,6-trimethyl-2-(3-methylbuta-1,3-dienyl)-3 oxatricyclo [5.1.0.0(2,4)] octane (3.90% w/w), valencene (2.8% w/w) and calarene (2.41% w/w) respectively. While the major compounds reported by Saraswathy et al. was androstan-17-one,3-ethyl-3-hydroxy-(5α) (24.69% w/w), (-)-spathulenol (9.03% w/w), 3-isopropyltricyclo undec-3-en-10-ol (9.03% w/w), z-valerenyl acetate (7.20% w/w), 1h-cycloprop(E) azulene,decahydro-1,1,7- (5.97% w/w), megastigma-4,6(e),8(z)-triene (5.84% w/w), 1h-cycloprop(e) azulen-7-ol (5.20% w/w), 3-cyclohexane-1-methanol (4.44% w/w), azulene (2.64% w/w), α– bisabolol (2.49% w/w), 1,7,7-trimethy,-acetate (2.27% w/w), abieta-9(11),8(14),12-trien-12-ol (2.26% w/w), 1-naphthalenol (2.19% w/w), bicyclo[3.1.1.]hept-2-ene-2-methanol (2.16% w/w) and caryophyllene oxide (2% w/w) [30]. The major compounds reported by Sailaja et al. include α-costol acetate (15.7% w/w), α-costol (13.1% w/w), 10-acetylmethyl 3-carene (11.8% w/w), myrtenyl acetate (5.3% w/w), (e)-caryophyllene (4.4% w/w), 14-oxy-δ-cadineneti (3.7% w/w), β-gurjunene + ρ-cymen-7-yl acetate (3% w/w), ar-curcumene + γ-himachalene (2.9% w/w), eremophilone (2.7% w/w) and bornyl acetate (2% w/w) respectively [31]. Structural analysis of the individual compounds indicated that majority of them were terpenoids, i.e., the major components consists of a mixture of bicyclic monoterpenoides, sesquiterpenoid, aromatic hydrocarbon, diterpene and triterpene. The methodology followed by the three authors for detecting the individual components of essential oil was not uniform. Saraswathy et al. used shade dried root [30]. While Sailaja et al. has specified that one-week shade dried root was used [31]. However, both the authors did not mention the maturity of the source plant they have used for GC-MS/GC-FID analysis. While in the present study fresh root was harvested from 90 days old plant following the standardized field cultivation practices [17]. Hence, maximum number of individual compounds reported in the present investigation. Essential oils are complex mixtures of volatile compounds mainly composed of terpenes which include monoterpenes (hydrocarbon and oxygenated monoterpenes), and sesquiterpenes (hydrocarbon and oxygenated sesquiterpenes). Besides, phenolic compounds are also present [32]. Essential oil showed high variability of their composition in qualitatively and quantitatively. This variability is attributed by many factors such as

soil type, seasonal variations, plant organ, plant maturity, geographical origin, harvesting time even at harvest time during the same day and genetics. In addition, extraction method and environment also greatly influence its individual component yield [32]. The essential oils showed a wide array of therapeutic activities and its additive, antagonistic and synergetic effects are well demonstrated [33].

***In Silico* Screening**

The recent investigations revealed that phyto-medicine is a potential therapeutic solution to treat diseases with multi-factorial causation like type II diabetes and also effective to control rapidly mutating pathogens/health condition linked to drug resistance. The modern therapeutic 'one drug' 'one target' concept offers off-target side effects and proven to be useful to single gene disorders. While disease often results from multi-factorial conditions involving breakdown of robust physiological system due to multiple genetic or environmental factors loading to the establishment of robust disease condition [34]. Such complex disorders are more likely to be healed or alleviated through simultaneous modulation of multiple targets [35]. Many plant derived drugs used in modern medicine find multiple therapeutic activity after long term usage, for example the salicylic acid originally isolated from willow tree and later modified to aspirin which has been widely used as a painkiller, later find many therapeutic activities such as coronary artery disease, heart attack, stroke, etc. and now aspirin is considered as a wonder drug. It is also well acknowledged that instead of using combination of drugs molecules hitting more than one targets may possess in principle a safer profile [36,37]. In these backdrops, in the present investigation six targets which can control the production of insulin and maintain the glucose level in human body were selected. The structural and functional features of the selected targets are as follows.

Target Proteins - Sstructural and Ffunctional Pproperties

11β-hydroxysteroid dehydrogenase type 1 (11β-HSD1): It is an enzyme that catalyzes the intercellular functionally inert glucocorticoid precursors (cortisone) to active glucocorticoids (cortisol) within insulin target tissues, thereby regulating metabolic changes such as insulin resistance and hyperglycemia. Iinhibition of this enzyme may offer a new therapeutic approach to managing type II diabetes mellitus [38]. The human 11 β-HSD1 contains 292 amino acids with molecular mass around 34 kDa. Its structures are similar overall, although the hydrophobic substrate binding pocket, predominantly lined by non-polar residues and with lower sequence conservation than other regions, shows some variability between species, accounting for the species specificity of inhibitors. It is a nicotinamide adenine dinucleotide phosphate (NADPH)-dependent enzyme that contains an N-terminal nucleotide cofactor-binding domain and a catalytic active site in its central region. The catalytic active site of the enzyme contains tyrosine (Tyr183) and lysine (Lys187) residues with the other two residues, Asn143 and Ser170 [39,40]. The protein consists of 52% helices, 23% beta sheets, 23% coils and 1% with a mean H-bond distance of 2.2 Å and mean H-bond energy -1.8 kj/mol. The crystal structure (PDB ID 1XU7) includes 3-[(3-cholamidopropyl) dimethylammonio]-1-propane sulfonateas the ligand molecule. There are two hydrogen bonds, TYR177 OH–O1 and TYR183 OH–O3, directly from the protein to the ligand.

Dipeptidyl peptidase IV (DPP IV): Dipeptidyl peptidase IV (DPP IV) is serine peptidases with many physiological functions and is widely distributed, existing both as a membrane-anchored cell-surface peptidase and as a smaller soluble form in blood plasma [41]. DPP-4 is a dimer of two identical sub units, each contains two domains: an N-terminal β-propeller domain and a C-terminal α/β-hydrolase domain. The two domains form a large cavity that houses the active site. The α/β-hydrolase domain is involved in dimerization, and the β-propeller domain is involved in both the dimeric and tetrameric interactions. Both the cell-surface and soluble forms of DPP-4 are catalytically active as dimers. Access to the cavity, and thus to the active site, is via an opening in the centre of the β-propeller or through the larger opening between the propeller and hydrolase domains [42,43]. Essential to the catalytic activity of DPP-4 are residues Ser630, Asp708 and His740 of the catalytic triad, Tyr547 in the hydrolase domain, and Glu205 and Glu206 in the β-propeller domain plays vital role in regulation of incretins hormone, the most important substrates of DPP-IV. Functionally, it selectively removes N-terminal dipeptides from substrates containing proline or alanine as the second residue and there by convert them into inactive form [45]. The protein consists of 14% helices, 45% beta sheets, 40% coils with a mean H-bond distance of 2.2 Å and means H-bond energy -1.9kj/mol. The crystal structure (1PFQ) contains 2-acetamido-2-deoxy-beta-D-glucopyranose as a co-factor.

Protein-tyrosine phosphatase 1B (PTP1B): It is a unique enzyme that is included in the protein tyrosine phosphatase (PTP) family. It is encoded by the (Tyrosine-protein phosphatase non-receptor type 1) PTPN1 gene in humans. PTPs are characterized by a conserved active site sequence (H/V) C(X) 5R(S/T), called the PTP signature motif, in which the cysteine residue functions as a nucleophile and is essential for catalysis [45]. This monomeric enzyme contains 435 amino acid residues and a molecular weight of 50kDa. It contains an N-terminal catalytic domain, two proline-rich sequences and a C-terminal hydrophobic region. The active site of PTP1B is located in the P fold of 214-221 residues, in which Cys215 and Arg221 are critical to its phosphatase catalytic sites. The active site His214–Arg221 lies within the pTyr substrate binding region.

The essential reduced Cys-215 lies within this sequence. The three-dimensional view is the WPD (tryptophan, proline, aspartic acid) loop (Thr177–Pro185). The WPD loop is a flexible region which is in 'open' conformation in the absence of any substrate and closes when the pTyr substrate binds with the region. Closure is essential for catalysis, and H-bonds forms between the amino acids Trp179 in the WPD loop and Arg 221 in the active site. Inhibitors which reduce the WPD loop mobility may block substrate binding and/or decrease catalytic activity. The S-loop, Ser201–Gly209, also influences WPD loop mobility and itself is inhibited by inhibitor binding [46]. The protein consists of 37% helices, 24% beta sheets, 38% coils with a mean H-bond distance of 2.2 Å and means H-bond energy -1.8kj/mol. The crystal structure (2QBQ) contains 4-bromo-3-(carboxymethoxy)-5-{3-[(3,3,5,5-tetramethylcyclohexyl) amino] phenyl} thiophene-2-carboxylic acid as a ligand. There are five H-bonds directly from the protein to the ligand with amino acid residues such as GLN266, PHE182, LYS120 and ARG221.

Human pancreatic alpha-amylase (PDB ID: 2QV4): The enzyme α-amylase catalyzes the hydrolysis of α-1,4glycosidic linkages in carbohydrates, thereby converting the starch and related polysaccharides into absorbable monosaccharides. It is considered as one of the major therapeutic targets of type II diabetes. Amylases are members of the glycoside hydrolases family [47,48]. The crystal structure of human pancreatic α-amylase consists of 496 amino acids,117 (23%) helices and 157(31%) β sheets, 221(44%) coils with a mean H-bond distance of 2.2 Å and mean H-bond energy -1.8kj/mol. It has a molecular weight of 55887.55 kDa and a theoretical pI value of 6.45. It has a single polypeptide chain, which is known to fold into three domains. Domain A is a $(\beta/\alpha)_8$ barrel which binds a chloride ion as an allosteric molecule. The functional active site is a "V"-shaped depression located at the C-terminal end of the $(\beta/\alpha)_8$ barrel. Domain B is occupied between the third β -strand and the helix of the first domain, binds a calcium ion and appears to be needed for the structural stability of an active site loop. Domain C, the putative starch-binding domain, is an eight-stranded β-sheet domain at the C-terminal end of the enzyme [49]. The target protein is predicted as a stable protein with an instability index of 23.79 and an aliphatic index of 68.17 using ProtParam. The active site of the protein consists of 23 amino acid residues. The crystal structure(2QV4) contains 4,6-dideoxy-4-{[(1S,4R,5R,6S)-4-{[alpha-D-glucopyranosyl-(1->4)-alpha-D-glucopyranosyl-(1->4)-alpha-D-glucopyranosyl]oxy}-5,6-dihydroxy-3-(hydroxymethyl) cyclohex-2-en-1-yl]amino}-alpha-D-glucopyranose as a ligand molecule.

Human lysosomal acid-alpha-glucosidase (PDB ID: 5NN8): Alpha-glucosidase is a member of the glycoside hydrolase family GH31, present in the brush border membrane of the intestines and functionally hydrolyzes both a-1,4 and a-1,6 linkages of oligosaccharides, and converts them into monosaccharides [50]. It catalyzes the release of glucose from glycogen, with slowing at branching points [51-52]. Alpha glucosidase is an important drug target involved in the mechanisms of diabetes mellitus and its inhibition controls hyperglycemia. The crystal structure of α-glucosidase consists of 872 amino acids, which form 164(19%) helices and 345(40%) beta sheets, 335(39%) coils with a mean H-bond distance of 2.2 Å and mean H-bond energy -1.9kj/mol. It has a molecular weight of 96882.03 kDa and a theoretical pI value of 5.29. The target protein is predicted as a stable protein with an instability index of 45.30 and an aliphatic index of 83.08 using ProtParam. The active site of the protein consists of 23amino acid residues. The crystal structure (5NN8) contains alpha-acarbose as a ligand.

Insulin receptor tyrosine kinase: The phosphorylated, activated form of the insulin receptor is an α2β2 trans-membrane glycoprotein with intrinsic protein tyrosine kinase activity. Binding of insulin to the extracellular α-chains results in auto-phosphorylation of specific tyrosine residues in the cytoplasmic region of β chain, which is critical for kinase activity [53]. The insulin receptor is effectively involved in the regulation of glucose homeostasis and is considered as a potential target for the screening for anti-diabetic activity [54]. Inactivation of insulin receptor by knocking out its gene results in the loss of insulin secretion and glucose tolerance. The studies have evidently described the role of IR in glucose homeostasis and showed its importance in the treatment of DM [55]. The crystal structure of insulin receptor tyrosine kinase consists of 348 amino acids, which form 100 (32%) helices and 71(23%) beta sheets, 135(44%) coils with a mean H-bond distance of 2.2 Å and mean H-bond energy -1.9kj/mol. It has a molecular weight of 39387 kDa and a theoretical pI value of 5.41. The target protein is predicted as a stable protein with an instability index of 43.77 and an aliphatic index of 76.15 using ProtParam. The active site of the protein consists of 23amino acid residues. The crystal structure (1IR3) contains phosphoaminophosphonic acid-adenylate ester as a ligand.

Molecular Docking

The docking between each of the selected targets, namely 11β-HSD1, DPP IV, PTP1B, human pancreatic alpha-amylase, human lysosomal acid-alpha-glucosidase and phosphorylated insulin receptor tyrosine kinase and 78 phytochemicals determined through GC-MS analysis of the root derived essential oil of *Plectranthus vettiveroides* were carried out in AutoDockVina. As followed by many authors, the docked structures having ΔG bind less than -6 kcal/mol were selected as hit molecules [56,57]. The number of hit molecules obtained against each target protein such as 11β-HSD1, DPP IV, PTP1B, human pancreatic

alpha-amylase, human lysosomal acid-alpha-glucosidase and phosphorylated insulin receptor tyrosine kinase was 52, 61, 63, 57, 70, and 40 respectively and the docking score against each target protien were depicted in Table 1. Out of 78 phytochemicals screened, 37 have shown binding energy ≤ -6 kcal/mol against all the tested targets. The top five hit molecules obtained against each target protein with binding energy value and interaction details were depicted in Table 2 and its docked images were depicted in Figure 2. All the top ranked hits obtained against each target showed inhibitory effect (binding energy ≤ -6 kcal/mol) on all the targets. The compound dehydroabietan was found to be among the top five hits against all targets but this phytochemical didn't show any H-bonds with none of the targets. The compound 4-(1-adamantane carboxamido)-2-ethyl-6-methyl-3-pyridyl1 adamantane carboxylate was found among the top five hits except against PTP1B, however it showed binding energy ≤ -7.3 kcal/mol with PTP1B. The compound has an H-bond with alpha glucosidase and two H-bonds with insulin receptor and no H-bond with other targets. Similarly, the compound dronabinol was found to have top five hits against the targets except alpha glucosidase. However, this compound showed binding energy ≤ -7.9 kcal/mol with alpha glucosidase. Dronabinol showed three H-bonds with 11β-HSD1, one H-bond with DPP4, PTP1B and alpha amylase, and two H-bonds with insulin receptor. Trans-totarol was found to be the top five hits against the targets except against PTP1B and insulin receptor, but this molecule showed binding energy ≤ -5.6 and ≤ -6.9 kcal/mol respectively against these two targets. Trans-totarol showed one H-bond with DPP4 and alpha amylase and no H-bond with the other two targets. The compound bicycle [4.4.0] dec-5-ene, 1,5-dimethyl-3-hydroxy-8-(1-methylene-2-hydroxyethyl-1) was found to be the top five hits against 11β-HSD1 and PTPIB. It has two H-bonds with 11β-HSD1 and no H-bond with PTPIB, however, its binding energy with other target proteins was ranging from -6.6 to -8 kcal/mol. The compound aacetate, [6-(acetyloxy)-5,5,8a-trimethyl-2-methyleneperhydro-1-naphthalenyl] methyl ester was the top five hits against DPP4, alpha amylase and insulin receptor, however, it showed binding energy ≤ -6.1kcal/mol with all other targets. It showed two H-bonds with DPP4 and alpha amylase, and no H-bonds with insulin receptor. Alpha-longipinene and ylangene belong to the top five hits against PTP1B but these molecules have not shown H-bonds with the targets. Similarly, alpha-himachalene and 6-(1-hydroxymethylvinyl)-4,8a-dimethyl-3,5,6,7,8,8a-hexahydro-1H-naphthalen-2-on belong to the top five hits against alpha glucosidase without any H-bond interaction. The compound γ-gurjunenepoxide was the top five hits against insulin receptor without H-bond interaction.

Table 2: Binding interaction details of five top ranked hits with selected targets.

Target Protein	Phytochemicals	ΔG Bind (kcal/mol)	H bond interaction	Bond length (°A)	Hydrophobic interactions
11B HSD	4-(1-Adamantanecarboxamido)-2-ethyl-6-methyl-3-pyridyl 1-adamantanecarboxylate ($C_{30}H_{40}N_2O_3$)	-9.8	Nil		Ala172, Val180, Lys187, Leu215, Ile218, Ala223, Leu217, Val227, Val231, Tyr177, Leu217
	Dehydroabietan ($C_{20}H_{30}$)	-8.3	Nil		Ile46, Lys44, Ile121, Leu215
	Trans-totarol ($C_{20}H_{30}O$)	-8.2	Nil		Lys44, Ile121, Ile46
	Dronabinol	-8.2	Arg66:HH12...O23: Lig Gly41:CA…O17: Lig His120:CA…O:17: Lig	2.57 3.07 3.47	Lys44, Ile121, Arg66, Val142
	Bicyclo[4.4.0]dec-5-ene, 1,5-dimethyl-3-hydroxy-8-(1-methylene-2-hydroxyethyl-1) ($C_{15}H_{24}O2$)	-7.4	Ser169:O…H33: Lig Leu215:O…H33: Lig	2.68 2.90	Ile46, Ile215, Ala223, Ile218, Ile121
DPP 4	Dehydroabietan	-8.4	Nil		Trp59, Tyr62, Ala198, His101, His299
	4-(1-Adamantanecarboxamido)-2-ethyl-6-methyl-3-pyridyl 1-adamantanecarboxylate ($C_{30}H_{40}N_2O_3$)	-8.3	Nil		Tyr62, Ala198, Ile235, His201, Leu162, Tyr151, Trp59, His305
	Trans-totarol ($C_{20}H_{30}O$)	-7.7	Arg195:HH21-O:21: Lig	2.22	Tyr62, His299, Trp58, Trp59, Leu165
	Dronabinol	-7.7	His101: HE-O23: Lig	2.43	Tyr62, Val98, Trp59 Ala198 His299
	Acetate, [6-(acetyloxy)-5,5,8a-trimethyl-2-methyleneperhydro-1-naphthalenyl] methyl ester ($C_{19}H_{30}O_4$)	-7.4	Arg195:HH21—O3: Lig Ala198:HN---O3: Lig	2.24 2.02	Trp58, Tyr62, His305
PTP1B	Bicylo[4.1.0]heptane, 7-bicyclo[4.1.0]hept-7-ylidene	-8.6	Nil		Leu110, Trp179, Phe182, Ala217

	Alpha-Longipinene	-8.5	Nil		Trp179, Leu110, Ala217, Phe182
	Dronabinol	-8.5	Lys120:HZ2—O23: Lig	2.35	Val49, Tyr46, Phe182, Trp179, Ala217
	Dehydroabietan	-8.2	Nil		Val49, Phe182, Tyr46, Ala217
	Ylangene	-8	Nil		Tyr46, Phe182, Ala217
Alpha amylase	Dehydroabietan	-9.1	Nil		Tyr62, Ala198, Trp59, Tyr62, His101, His299
	4-(1-Adamantanecarboxamido)-2-ethyl-6-methyl-3-pyridyl 1-adamantanecarboxylate	-8.7	Nil		Trp59, Tyr151, Leu162, His201, Ile235, Ala198, Tyr62, His305
	Dronabinol	-8.5	His:101: HE—O23	2.43	Tyr62, Ala198, Val98, Trp59, Tyr62, His101, His229
	Trans-totarol ($C_{20}H_{30}O$)	-8	Arg195:HH21—O21	2.22	Tyr62, Trp58, Trp59, Leu165, His299
	Acetate, [6-(acetyloxy)-5,5,8a-trimethyl-2-methyleneperhydro-1-naphthalenyl] methyl ester ($C_{19}H_{30}O_4$)	-7.5	Arg195:HZ21—O3: Lig Ala198:HN—O3: Lig	2.24 2.02	Trp58, Tyr62, His305
Alpha glucosidase	Trans-totarol	-9.2	Nil		Ala28, Trp481, Trp516, Met519, Phe649, Leu650
	Dehydroabietan	-8.8	Nil		Trp516, Trp613, Phe649; Leu650, Ala284, Arg600
	α-Himachalene	-8.6	Nil		Ile441, Trp481, Trp516, Met519, Trp613, Phe649
	4-(1-Adamantanecarboxamido)-2-ethyl-6-methyl-3-pyridyl 1-adamantanecarboxylate	-8.1	Arg60HH11—O11: Lig	2.20	Phe649, Ala284, Ile441, Trp481, Trp516
	6-(1-Hydroxymethylvinyl)-4,8a-dimethyl-3,5,6,7,8,8a-hexahydro-1H-naphthalen-2-on	-8.1	Nil		Ala284, Phe649, Met519, Leu650
Insulin receptor	4-(1-Adamantanecarboxamido)-2-ethyl-6-methyl-3-pyridyl 1-adamantanecarboxylate	-8.1	Ser1270; HG—O11; Lig HIS1268: CE—O1: Lig	2.49 2.77	Val1274, HIS1057 His1268, Phe1144, Phe1271
	Dehydroabietan	-7.5	Nil		Leu1045, Val1065, Val1074, Val1032, Arg1041
	Dronabinol	-7.4	Asp1227:HN—O17: Lig GLN2110:O—H53: Lig	2.5 2.05	Phe1221, Pro1231, LE1213 Trp1200, Leu1228
	Acetate, [6-(acetyloxy)-5,5,8a-trimethyl-2-methyleneperhydro-1-naphthalenyl] methyl ester ($C_{19}H_{30}O_4$)	-7	Nil		Met1112, His1268
	γ-Gurjunenepoxide-(2)	-6.9	Nil		Val1010, Ala1028, Met1139, Leu1002, Met1079Lys1030, Met1076

Molecular Property and Drug-likeness Score

The molecular property analysis of the ten top ranked hits using the tool MOLSOFT is depicted in Table 3, which was based on Lipinski report [58]. Out of ten hits, five of them violated LogPvalue and the hydrogen donors and acceptors were absent in four hits and none of the compounds exceeded the number of hydrogen donors and acceptors. Only one molecule showed a positive drug-likeness score whereas all the other nine molecules showed negative drug-likeness scores. However, among those except two compounds, viz. bicycle [4.1.0] heptane, 7-bicyclo [4.1.0] hept-7-ylidene and α-himachalene, the negative drug-likeness scores were close to zero, which is acceptable. The compound 4-(1-adamantanecarboxamido)-2-ethyl-6-methyl-3-pyridyl 1-adamantanecarboxylate has a promising drug-likeness score, which is a common lead compound against five

of the six selected target proteins. In general, the Lipinski's rule of five is not applicable to natural compounds [59].

ADMET Property Analysis

The ADMET properties of the top ten hits were depicted in table 4. The results indicated that all top ranked molecules have good absorption parameters. All hits showed Caco2 permeability value >0.90 except 4-(1-adamantanecarboxamido)-2-ethyl-6-methyl-3-pyridyl 1-adamantanecarboxylate, which has Caco2 permeability value 0.675. All hit molecules have good intestinal absorption value; indicate that they can be effortlessly absorbed through the human intestine. In distribution parameters, except the compound aacetate, [6-(acetyloxy)-5,5,8a-trimethyl-2-methyleneperhydro-1-naphthalenyl]methyl ester, all others have good BBB permeability value and the majority of the compound penetrate CNS membrane. None of the compound acts as CYP2D6 substrates and inhibitors of CYP2D6 and CYPCA4. Out of ten compounds, only alpha-himachalene acts as inhibitor of CYP2C9 and CYP2C19. Out of the ten compounds except acetate, [6-(acetyloxy)-5,5,8a-trimethyl-2-methyleneperhydro-1-naphthalenyl] methyl ester, all others did not

act as renal OCT2 substrate. None of the compounds exhibits AMES toxicity and hepatotoxicity. The overall ADMET results indicated that all the compounds can be accepted as drug molecules.

Table 3: Molecular property and drug-likeness analysis of the lead molecules using MOLSOFT

Compound Name	Molecular weight	HBA	HBD	MolLoP	MolLog S	MolPSA	BBB Score	Drug-likeness score
4-(1-Adamantanecarboxamido)-2-ethyl-6-methyl-3-pyridyl 1-adamantanecarboxylate ($C_{30}H_{40}N_2O_3$)	476.30	4	1	7.36	-5.67	52.94	3.87	1.28
trans-Totarol (C_{20} H_{30} O)	286.23	1	1	5.94	-5.60	16.63	4.81	-0.26
Dehydroabietan (C_{20} H_{30})	270.23	0	0	6.52	-6.16	0.00	1.82	-0.12
Bicylo[4.1.0]heptane, 7-bicyclo[4.1.0]hept-7-ylidene (C_{14} H_{20})	188.16	0	0	4.44	-4.33	0.00	1.22	-1.44
α-Himachalene (C_{15} H_{24})	204.19	0	0	5.30	-5.16	0.00	1.26	-1.24
Dronabinol (C_{21} H_{30} O_2)	314.22	2	1	7	-5.89	23.66	4.91	-0.05
6-(1-Hydroxymethylvinyl)-4,8a-dimethyl-3,5,6,7,8,8a-hexahydro-1H-naphthalen-2-one ($C_{15}H_{22}O2$)	234.16	2	1	3.06	-2.47	30.82	4.29	-0.19
Ylangene (C_{15} H_{24})	204.19	0	0	4.89	-4.87	0.00	1.26	-0.89
Acetate, [6-(acetyloxy)-5,5,8a-trimethyl-2-methyleneperhydro-1-naphthalenyl] methyl ester (C_{19} H_{30} O_4)	322.21	4	0	4.53	-4.20	41.79	3.81	-0.45
Bicyclo[4.4.0]dec-5-ene, 1,5-dimethyl-3-hydroxy-8-(1-methylene-2-hydroxyethyl-1)-(C_{15} H_{24} O_2)	236.18	2	2	3.14	-2.4	33.19	4.26	-0.31

Figure 2: Docking between the target proteins and the best hit molecules: 1a. 11β-HSD1 and 4-(1-Adamantanecarboxamido)-2-ethyl-6-methyl-3-pyridyl 1-adamantanecarboxylate 1b.Ligand interaction with 11β-HSD1; 2a.DPP IV and dehydroabietan 2b.Ligand interaction with DPP IV; 3a.Human lysosomal acid alpha-glucosidase and trans-totarol, 3b.Ligand interaction with alpha-glucosidase; 4a.Human pancreatic alpha-amylase and dehydroabietan 4b.Ligand interaction with alpha-amylase; 5a. PTP1B and Bicylo[4.1.0]heptane, 7-bicyclo[4.1.0]hept-7-ylidene, 5b. Ligand interaction with PTP1B; 6a. Phosphorylated insulin receptor tyrosine kinase and 4-(1-Adamantanecarboxamido)-2-ethyl-6-methyl-3-pyridyl 1-adamantanecarboxylate, 6b. Ligand interaction with insulin receptor tyrosine kinase.

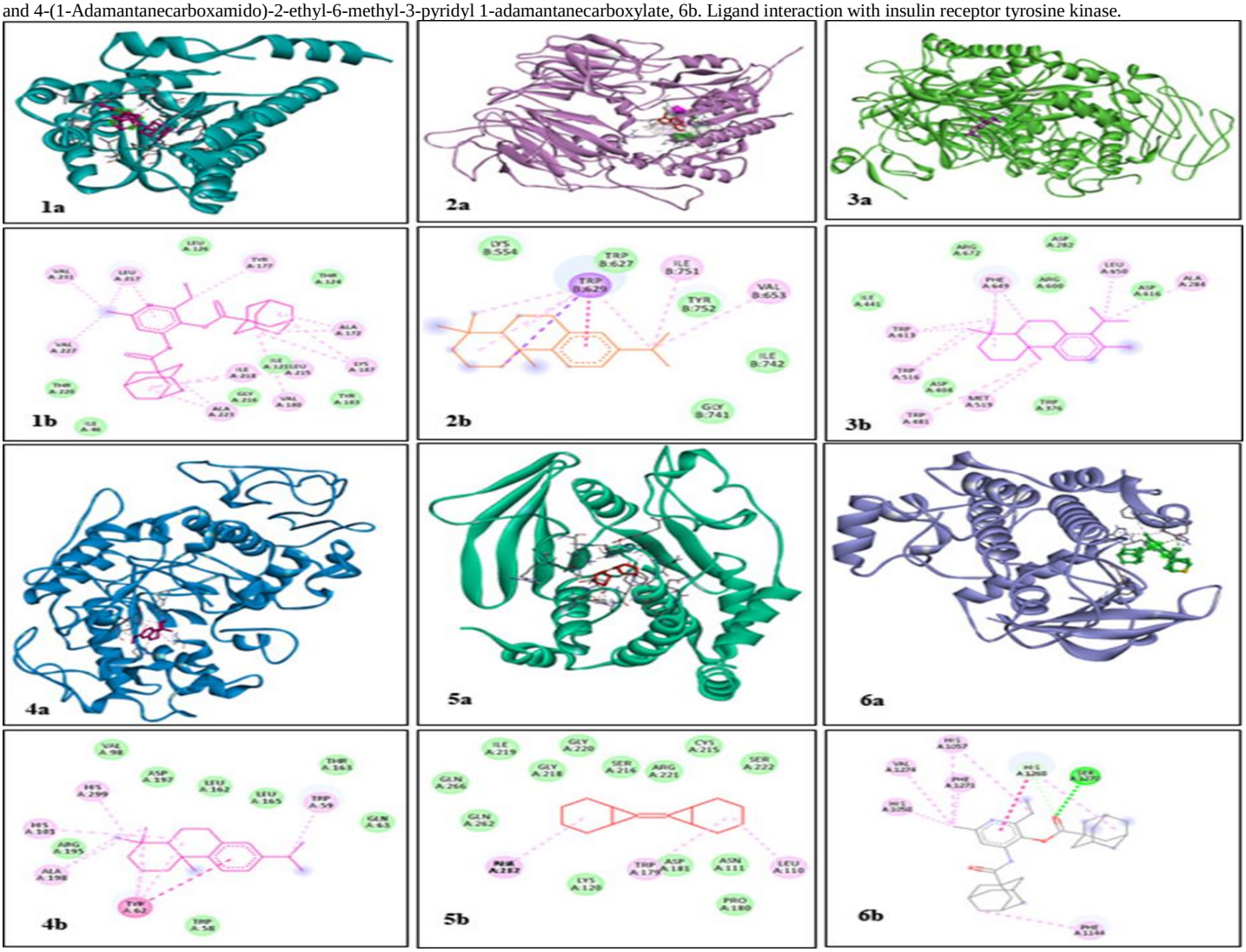

Table 4: Absorption, distribution, metabolism, excretion toxicity (ADMET) property analysis of the top ten hits

	Property	4-(1-Adamantanecarboxamido)-2-ethyl-6-methyl-3-pyridyl 1-adamantanecarboxylate	trans-Totarol	Dehydroabietan	Bicyclo[4.1.0]heptane, 7-bicyclo[4.1.0]hept-7-ylidene	alpha-Himachalene	Dronabinol	6-(1-Hydroxymethylvinyl)-4,8a-dimethyl-3,5,6,7,8,8a-hexahydro-1H-naphthalen-2-one	Ylangene	Acetate, [6-(acetyloxy)-5,5,8a-trimethyl-2-methyleneperhydro-1-naphthalenyl] methyl ester	Bicyclo[4.4.0]dec-5-ene, 1,5-dimethyl-3-hydroxy-8-(1-methylene-2-hydroxyethyl-1)-
Absorption	Caco2 permeability (logPapp in 10^{-6} cm s^{-1})	0.675	1.559	1.476	1.384	1.418	1.519	1.51	1.374	1.447	1.655
	Intestinal absorption (%)	91.851	92.769	93.831	95.771	94.556	93.091	94.818	96.221	97.343	93.961
	Skin permeability ($logK_p$)	-2.729	-2.65	-2.465	-2.379	-1.641	-2.538	-2.34	-2.225	-2.981	-2.7
	P-Glycoprotein substrate	Yes	No	No	No	No	No	No	No	No	No
	P-Glycoprotein I	Yes	No	No	No	No	No	No	No	Yes	No
	P-Glycoprotein II	Yes	Yes	No	No	No	No	No	No	No	No
Distribution	VDss (log L kg^{-1})	-0.625	1.159	1.4 .	0.632	0.648	0.95	0.281	0.806	0.093	0.272
	BBB permeability (logBB)	-0.135	0.547	0.669	0.891	0.731	0.865	0.078	0.887	-0.055	0.053
	CNS permeability (logPS)	-1.169	-1.352	-1.016	-1.106	-2.322	-2.133	-2.303	-1.659	-2.744	-2.403
Metabolism	CYP2D6 substrate	No	No	No	No	No	No	No	No	No	No
	CYP2C19 inhibitor	No	No	No	No	Yes	No	No	No	No	No
	CYP2C9 inhibitor	No	No	No	No	Yes	No	No	No	No	No
	CYP2D6 inhibitor	No	No	No	No	No	No	No	No	No	No
	CYP3A4 inhibitor	No	No	No	No	No	No	No	No	No	No
Excretion	Total clearance (log ml mim^{-1} kg^{-1})	-0.17	0.704	0.961	1.032	1.1	0.756	1.221	0.95	1.074	1.208
	Renal OCT2 substrate	No	No	No	No	No	No	No	No	Yes	No
Toxicity	AMES toxicity	No	No	No	No	No	No	No	No	No	No
	Max. tolerated dose (log mg kg^{-1} day^{-1})	0.563	-0.21	-0.134	-0.421	0.407	-0.138	-0.004	-0.302	0.037	0.03
	hERG I inhibitor	No	No	No	No	No	No	No	No	No	No
	hERG II inhibitor	No	Yes	Yes	No	No	No	No	No	No	No
	Hepatotoxicity	No	No	No	No	No	No	No	No	No	No
	Skin sensitisation	Yes	Yes	No	No	Yes	No	Yes	No	No	Yes
	T. pyriformis toxicity (log µg L^{-1})	0.842	0.285	0.95	0.931	1.33	0.763	1.495	1.122	1.136	1.262
	Minnow toxicity (log mM)	-1.475	-0.766	-1.667	0.091	0.654	0.768	1.078	0.128	0.928	1.305

CONCLUSION

The overall results indicated that the essential oil contains a plethora of chemical molecules with an inhibitory effect on DM multi-targets. The phytochemical analysis revealed that the major component of the essential oil is terpenoids, which are highly volatile and showed structural instability/variability. However, the basic structural components of all the individual phytochemicals of the essential oil are the same. The study also revealed that no toxicity is induced by the components of the essential oil. In this context, instead of proposing an individual chemical constituent the essential oil as such can be recommended against DM since the individual, synergistic and cumulative effect of phytochemicals may concomitantly inhibit multi-targets of DM and act as an effective drug.

ACKNOWLEDGMENT

The authors thank CSIR for providing a Junior Research Fellowship to carry out this research work leading to a Ph.D. We also thank Director, KSCSTE-Jawaharlal Nehru Tropical Botanic Garden and Research Institute for providing the facilities and all other support.

DECELERATION OF CONFLICT OF INTEREST

The author(s) confirms that this article's content has no conflict of interest.

REFERENCES

1. Piero MN, Nzaro GM, Njagi JM, 2015. Diabetes mellitus - a

devastating metabolic disorder. Asian Journal of Biomedical and Pharmaceutical Sciences 4(40), Pages- 1-7. DOI: 10.15272/ajbps.v4i40.645.

2. SamreenRiaz, 2009. Diabetes mellitus. Scientific Research and Essays 4(5), Pages-367-373.

3. Bastaki S, 2005. Diabetes mellitus and its treatment. International Journal of Diabetes and Metabolism 13(3), Pages-111-134. Doi: 10.1159/000497580.

4. Deshmukh, Chinmay D, Anurekha Jain, 2015. Diabetes Mellitus: A review. International Journal of Pure & Applied Bioscience 3(3), Pages- 224-230.

5. Katsarou A, Gudbjörnsdottir S, Rawshani A, et al, 2017. Type 1 diabetes mellitus. Nature Review Disease Primers 3(1), Pages-1-7. Doi: 10.1038/nrdp.2017.16.

6. Subramanian S, Baidal D, 2021. The management of type 1 diabetes. Endotext, MD Text.com, Inc., Pages-.1-91.

7. Walker JM, Harrison FE, 2015. Shared neuropathological characteristics of obesity, type 2 diabetes and alzheimer's disease: Impacts on cognitive decline. Nutrients 7(9), Pages-7332-7357.

8. De Fronzo RA, Ferrannini E, Groop L, et al, 2015. Type 2 diabetes mellitus. Nature Review Disease Primers 1(1), Pages-1-22. Doi: 10.1038/nrdp.2015.19.

9. Marín-Peñalver JJ, Martín-Timón I, Sevillano-Collantes C, et al, 2016. Update on the treatment of type 2 diabetes mellitus. World Journal of Diabetes 7(17), Pages- 354-395. Doi: 10.4239/wjd.v7.i17.354.

10. Grover JK, Yadav S, Vats V, 2002. Medicinal plants of India with anti-diabetic potential. Journal of ethnopharmacology 81(1), Pages- 81-100. Doi: 10.1016/s0378-8741(02)00059-4.

11. Sreekumar S, Nisha NC, 2022. Plants are renewable source of medicine and nanoparticles: A review. In: OhnYahya I. Elshimali and Charles R (edition 8) current aspects in pharmaceutical research and development bp international UK, pp. 44-56. Doi:10.9734/bpi/caprd/v8.

12. Nikumbh KK, Rupali A Patil, 2021. Some medicinal plants with anti-diabetic activity in experimental animals: A systematic review. Journal of medical pharmaceutical and allied sciences, IC 1 - I 1 (1910), Page 31-36. Doi: 10.22270/jmpas.IC1I1.1910.

13. Nisheeda BA, Safeer PM, Sreekumar S, et al, 2016. A review on Plectranthus vettiveroides: An endemic to South Indian high value aromatic medicinal plant. Journal of pharmacy and biological sciences 11(2), Pages- 1-11. Doi: 10.9790/3008-1102030111.

14. Kamal BS, Padmaja V, 2014. Evaluation of antimicrobial activity of various and volatile oil from the whole plant of Coleus vettiveroids KC Jacob: An *in vitro* study. International Journal of Pharmacy and Pharmaceutical Sciences 6(1), Pages-638-640.

15. Safeer PM, Sreekumar S, Krishnan PN, et al, 2013. Influence of soil texture and bed preparation on growth performance in Plectranthus vettiveroides. IOSR Journal of Agriculture and Veterinary Sciences 5(3), Pages- 41-45. Doi:10.9790/2380-0534145.

16. Shivananda TN, Mamatha B, Ganeshamurthy AN, 2007. Problems and prospects in cultivation of *Plecranthus vettiveroides* (KC Jacob) NP Singh & BD Sharma. limitations in identification, nomenclature, distribution and cultivation- a case study. Biomed 2(2), Pages-146-154.

17. Deepa V, Sreekumar S, Biju CK, 2018. *In silico* validation of anti-russell's viper venom activity in *Phyllanthus emblica* L. and *Tamarindus indica* L. International Journal of Pharmaceutical Sciences and Drug Research 10(4), Pages- 217-226. Doi: 10.25004/IJPSDR.2018.100403.

18. Nisha NC, Sreekumar S, Evans DA, et al, 2018. *In vitro* and *in silico* validation of anti-cobra venom activity and identification of lead molecules in *Aegle marmelos* (L.) Correa. Current Science 114(6), Pages-1214-1221.

19. Nandagopalan V, Gritto MJ, Doss A, 2015. GC-MS analysis of bioactive components of the methanol extract of *Hibiscus tiliaceus* Linn. Asian Journal of Plant Science & Research 5(3), Pages-6-10.

20. Asha KR, Priyanga S, Hemmalakshmi S, et al, 2017. GC-MS analysis of the ethanolic extract of the whole plant *Drosera indica* L. International Journal of Pharmacognosy and Phytochemical Research 9(5), Pages- 685-8. Doi: 10.25258/phyto.v9i2.8149.

21. Willard L, Ranjan A, Zhang H, et al, 2003. VADAR: A web server for quantitative evaluation of protein structure quality. Nucleic Acids Research 31(13), Pages- 3316-3319. Doi: 10.1093/nar/gkg565.

22. Johansson MU, Zoete V, Michielin O, et al, 2012. Defining and searching for structural motifs using DeepView/Swiss-PdbViewer. BMC Bioinformatics 13(173), Pages- 1-10. Doi: 10.1186/1471-2105-13-173.

23. Bolton EE, Wang Y, Thiessen PA, et al, 2008. PubChem: Integrated platform of small molecules and biological activities. Annual Reports in Computational Chemistry 31(4), Pages- 217-241. DOI: 10.1016/S1574-1400(08)00012-1.

24. Trott O, Olson AJ, 2010. AutoDockVina: Improving the speed and accuracy of docking with a new scoring function, efficient optimization, and multithreading. Journal of computational chemistry 31(2), Pages- 455-461. Doi: 10.1002/jcc.21334.

25. Joshi UP, Wagh RD, 2018. GC-MS analysis of phytochemical compounds present in the bark extracts of Ehretia laevis Roxb. International journal of research and development in pharmacy

& life science 7(6), Pages-3150-3154. Doi: 10.21276/IJRDPL.2278-0238.2018.7(6).3150-3154

26. Saraswathy A, Lavanya M, 2013. Chemical composition and antibacterial activity of the essential oil from the roots of Coleus vettiveroides KC Jacob. International journal of pharmacy and biological sciences 3(3), Pages- 212-217.

27. Sailaja GR, Sriramavaratharajan V, Murugan R, et al, 2021. Vasorelaxant property of Plectranthus vettiveroides root essential oil and its possible mechanism. Journal of ethnopharmacology 274, Pages- 1140-1148. Doi: 10.1016/j.jep.2021.114048.

28. Dhifi W, Bellili S, Jazi S, et al, 2016. Essential oils' chemical characterization and investigation of some biological activities: A critical review. Medicines 3(4) 25. Doi: 10.3390/medicines3040025

29. Chouhan S, Sharma K, Guleria S, 2017. Antimicrobial activity of some essential oils - present status and future perspectives. Medicines (Basel) 4(3), 58. Doi: 10.3390/medicines4030058.

30. Yildrim MA, Goh KI, Cusick ME, et al, 2007. Drug-target network. Nature Biotechnology 25 (10), Pages-1119–1126. Doi: 10.1038/nbt1338.

31. Talevi A, 2015. Multi-target pharmacology: possibilities and limitations of the "skeleton key approach" from a medicinal chemist perspective. Frontiers in pharmacology 6, Page- 205. Doi:10.3389/fphar.2015.00205.

32. Bolognesi ML, Cavalli A, 2016. Multi-target drug discovery and polypharmacology. Chem med chem 11(12), Pages- 1190-1192. Doi: 10.1002/cmdc.201600161.

33. Ramsay RR, Popovic-Nikolic MR, Nikolic K, et al, 2018. A perspective on multi-target drug discovery and design for complex diseases. Clinical and translational medicine 7(1), Pages- 1-4. DOI: 10.1186/s40169-017-0181-2.

34. Anderson A, Walker BR, 2013. 11β-HSD1 inhibitors for the treatment of type 2 diabetes and cardiovascular disease. Drugs 73(13), Pages-1385-1393. Doi: 10.1007/s40265-013-0112-5.

35. Almeida C, Monteiro C, Silvestre S, 2021. Inhibitors of 11β-hydroxysteroid dehydrogenase type 1 as potential drugs for type 2 diabetes mellitus - a systematic review of clinical and in vivo preclinical studies. Scientia pharmaceutica 89(1), Page- 5. DOI: 10.3390/scipharm89010005.

36. Chapman K, Holmes M, Seckl J, 2013. 11β-hydroxysteroid dehydrogenases: intracellular gate-keepers of tissue glucocorticoid action. Physiological reviews 93(3), Pages- 1139-1206. Doi: 10.1152/physrev.00020.2012.

37. Deacon CF, 2019. Physiology and pharmacology of DPP-4 in glucose homeostasis and the treatment of type 2 diabetes. Frontiers in endocrinology 10, Page-80. Doi: 10.3389/fendo.2019.00080.

38. Klemann C, Wagner L, Stephan M, et al, 2016. Cut to the chase: A review of CD26/dipeptidyl peptidase-4's (DPP4) entanglement in the immune system. Clinical & experimental immunology 185 (1), Pages-1-21. Doi: 10.1111/cei.12781.

39. Oefner C, D'Arcy A, Mac Sweeney A, et al, 2003. High-resolution structure of human apo dipeptidyl peptidase IV/CD26 and its complex with 1-[({2-[(5-iodopyridin-2-yl) amino]-ethyl} amino)-acetyl]-2-cyano-(S)-pyrrolidine. Acta Crystallographica Section D. Biological crystallography 59(7), Pages-1206-1212. Doi: 10.1107/S0907444903010059.

40. Thoma R, Löffler B, Stihle M, et al, 2003. Structural basis of proline-specific exopeptidase activity as observed in human dipeptidyl peptidase-IV. Structure 11(8), Pages- 947-959. Doi: 10.1016/S0969-2126(03)00160-6.

41. Jin T, Yu H, Huang XF, 2016. Selective binding modes and allosteric inhibitory effects of lupane triterpenes on protein tyrosine phosphatase 1B. Scientific reports 6(1), Page- 20766. Doi: 10.1038/srep20766.

42. Patel AM, Anand IS, Suva MA, 2014. Role of protein tyrosine phosphatase-1B inhibitors in type 2 diabetes mellitus. Journal of pharma scit tech 4(1), Pages-1-6.

43. Rydberg EH, Sidhu G, Vo HC, et al, 1999. Cloning, mutagenesis, and structural analysis of human pancreatic α-amylase expressed in Pichia pastoris. Protein science 8(3), Pages-635-643. Doi:10.1110/ps.8.3.635.

44. Henrissat B, Bairoch A, 1993. New families in the classification of glycosyl hydrolases based on amino acid sequence similarities. Biochemical journal 293(3), Pages-781-8. Doi 10.1042/bj2930781.

45. Nahoum V, Roux G, Anton V, et al, 2000. Crystal structures of human pancreatic α-amylase in complex with carbohydrate and proteinaceous inhibitors. Biochemical journal 346(1), Pages-201-8. Doi: 10.1042/bj3460201.

46. Roig-Zamboni V, Cobucci-Ponzano B, Iacono R, et al, 2017. Structure of human lysosomal acid α-glucosidase–a guide for the treatment of Pompe disease. Nature communications 8(1111), Pages-1-10. Doi: 10.1038/s41467-017-01263-3.

47. Van Hove JL, Yang HW, Wu JY, et al, 1996. High-level production of recombinant human lysosomal acid alpha-glucosidase in Chinese hamster ovary cells which targets to heart muscle and corrects glycogen accumulation in fibroblasts from patients with Pompe disease. National academy of sciences. 93(1), Pages- 65-70. DOI: 10.1073/pnas.93.1.65.

48. Adinortey CA, Kwarko GB, Koranteng R et al, 2022. Molecular structure-based screening of the constituents of Calotropis procera identifies potential inhibitors of diabetes mellitus target alpha glucosidase. Current Issues in Molecular Biology 44(2), Pages-963-987. Doi: 10.3390/cimb44020064.

49. Hubbard SR, 1997. Crystal structure of the activated insulin

receptor tyrosine kinase in complex with peptide substrate and ATP analog. The EMBO journal 16(18), Pages-5572-5581.Doi: 10.1093/emboj/16.18.5572.

50. Konidala SK, Kotra V, Danduga RC, et al, 2020. Coumarin-chalcone hybrids targeting insulin receptor: Design, synthesis, anti-diabetic activity, and molecular docking. Bioorganic chemistry 104(104207). Doi: 10.1016/j.bioorg.2020.104207.

51. Haeusler RA, McGraw TE, Accili D, 2018. Biochemical and cellular properties of insulin receptor signalling. Nature reviews molecular cell biology 19(1), Pages- 31-44. Doi: 10.1038/nrm.2017.89.

52. Shityakov S, Forster C, 2014. In silico predictive model to determine vector-mediated transport properties for the blood-brain barrier choline transporter. Advances and applications in bioinformatics and chemistry 2(7), Pages – 23 - 36. Doi: 10.2147/AABC.S63749.

53. Shefin B, Sreekumar S, Biju CK, 2021. Anti-tuberculosis activity in Punica granatum: *In silico* validation and identification of lead molecules. Indian journal of pharmaceutical sciences 83(2), Pages-316-330. Doi: 10.36468/pharmaceutical-sciences.778.

54. Lipinski CA, 2000. Drug-like properties and the causes of poor solubility and poor permeability. Journal of pharmacological and toxicological methods 44(1), Pages-235-49. Doi: 10.1016/S1056-8719(00)00107-6.

55. Ganesan A, 2008. The impact of natural products upon modern drug discovery. Current Opinion in Chemical Biology 12(3), Pages-306-317. Doi: 10.1016/j.cbpa.2008.03.016.

How to cite this article

Remya RP, Sreekumar S, Biju CK, 2022. *In silico* screening and identification of leads against multi-targets of type II diabetes in *Plectranthus vettiveroides*. Journal of medical pharmaceutical and allied science V 11 - I 5, Pages - 5268 – 5282. Doi: 10.55522/jmpas.V11I5.3957.